

Development of Gonio-photometric Imaging System for Recording Reflectance Spectra of 3D Objects

Kazutaka Tonsho, Yoshinori Akao, Norimichi Tsumura and Yoichi Miyake

Graduate School of Science and Technology, Chiba University
1-33 Yayoi-cho, Inage-ku, Chiba 263-8522, Japan

ABSTRACT

In recent years, it is required to develop a system for 3D capture of archives in museums and galleries. In visualizing of 3D object, it is important to reproduce both color and glossiness accurately. Our final goal is to construct digital archival systems in museum and internet or virtual museum via World Wide Web. To achieve our goal, we have developed gonio-photometric imaging system by using high accurate multi-spectral camera and 3D digitizer. In this paper, gonio-photometric imaging method is introduced for recording 3D object. 5-bands images of the object are taken under 7 different illuminants angles. The 5-band image sequences are then analyzed on the basis of both dichromatic reflection model and Phong model to extract gonio-photometric property of the object. The images of the 3D object under illuminants with arbitrary spectral radiant distribution, illuminating angles, and visual points are rendered by using OpenGL with the 3D shape and gonio-photometric property.

Keywords: Spectral Reflectance, Gonio-photometric Property, 3D Shape

1. INTRODUCTION

The internet museum, telemedicine, and network shopping on the World Wide Web have increased rapidly in recent years. In the present internet museum, however, color reproduction of the painting and 3D artifact is highly dependent on imaging devices. Therefore, it is required to record and reproduce the device independent color of the objects. In reproducing a real object on a display under arbitrary viewing conditions such as illuminant, illuminating angle, and visual point, an object model should contain both information of 3D shape and reflectance properties. A number of techniques have been developed for modeling 3D shapes and color of the object.

Sato, et.al.¹ developed a method for modeling of object reflectance properties, as well as object shapes, from multiple range and color images of real objects. In this method, the object shape is reconstructed by merging multiple range images of the rotated object. By using the reconstructed object shape and a sequence of color images of the object, parameters of a reflection model are estimated. The realistic images under arbitrary illuminating angles and visual points are synthesized. However, in this method, it is impossible to reproduce color of the object precisely under illuminant with arbitrary spectral distribution, since color is recorded by R, G, B 3 channels.

Haneishi et.al.²⁻⁴ proposed gonio-spectral imaging method based on dichromatic reflection model⁵ and Phong model⁶ from the set of multi-band images taken under different illuminating angles. However, it was not considered to record the shape information of the object.

In this study, we have developed gonio-photometric imaging system for recording the shape and reflectance spectra of 3D object by using highly accurate multi-spectral camera and 3D digitizer. The gonio-photometric characteristics of the object are taken by changing the angle of illuminant and also mapped onto the 3D shape. Reproducing the image of 3D object under any visual point is necessary to obtain gonio-photometric and spectral reflection properties at all points of 3D object. Then it becomes possible to reproduce the image using the reflection properties obtained from the image sequence under several visual points. The images of the 3D

E-mail: {tonsho, akao, tsumura, miyake}@icsd6.tj.chiba-u.ac.jp, Telephone & FAX: +81 43 290 3262 33

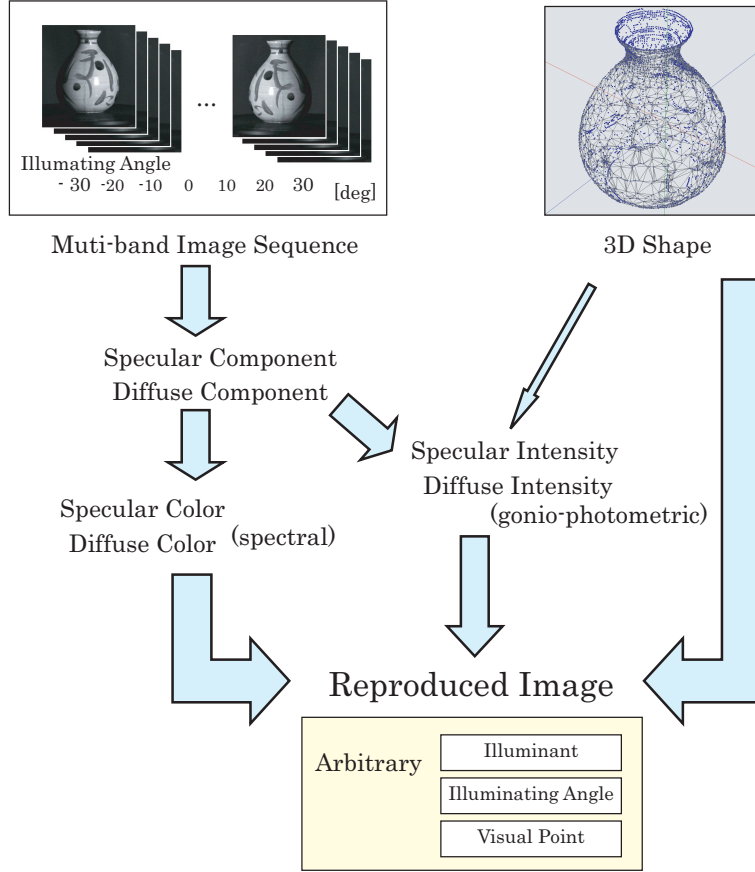


Figure 1: Diagram of obtaining reflection parameters and reproducing image under arbitrary condition.

object under arbitrary illuminants, illuminating angles, and visual points are rendered by using OpenGL with the information of the obtained 3D shape, gonio-photometric property, and spectral reflectance on the surface.

Figure 1 shows the flow for obtaining spectral and gonio-photometric reflectance property of 3D object and reproducing the image of object under arbitrary illuminants, illuminating angles, and visual points. It is assumed the surface of the object has a dichromatic reflection property⁵ in which light reflected from the surface is composed of two additive components, specular and diffuse reflections. The specular component has the same spectral distribution as illuminant, and the diffuse reflection component has inherent spectral distribution of the surface. Gonio-photometric intensities of these components are estimated using the multi-band image sequence taken under different illuminant angles to the normal line of 3D surface. These obtained properties are combined for synthesizing object images with realistic shading effects under arbitrary illuminants, illuminating angles, and visual points.

2. REFLECTANCE MODEL

2.1. Dichromatic Reflection Model

In computer vision and computer graphics, the dichromatic reflection model⁵ has been used to formulate the spectra of light reflected from object. For inhomogeneous dielectric materials such as plastics, it is known that the dichromatic reflection model represents the light reflected from object as the sum of specular and diffuse reflection component. The specular reflection component occurs at the interface between the object surface and air, and represents glossiness of the object. The spectral distribution of specular reflection component is

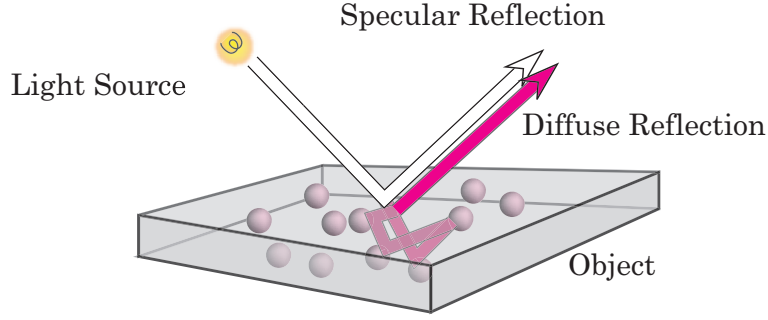


Figure 2: Schematic illustration of dichromatic reflection model.

equivalent to that of the illuminant. On the other hand, the diffuse reflection component is the light passed through the interface, scattered by colorants in the subsurface, and then emerged through the surface as shown in Figure 2. The spectral distribution therefore depends on both the illuminant and the colorants that construct the color of the surface.

Although the spectral characteristics are continuous, for convenience the discrete vector notation is introduced as follows,

$$\begin{aligned}\mathbf{L} &= \text{diag}[l_1, \dots, l_n] \\ \mathbf{o}(\mathbf{r}) &= [o_1(\mathbf{r}), \dots, o_n(\mathbf{r})]^T \\ \mathbf{f}(\mathbf{r}, \theta) &= [f_1(\mathbf{r}, \theta), \dots, f_n(\mathbf{r}, \theta)]^T,\end{aligned}$$

where \mathbf{L} is the spectral radiance of illuminant, $\mathbf{o}(\mathbf{r}, \theta)$ is the reflectance spectra of object at the coordinate \mathbf{r} and the geometric condition θ that decided from the angle of illuminant and visual point. According to the dichromatic reflection model, the spectral radiance $\mathbf{f}(\mathbf{r}, \theta)$ is described as the sum of specular and diffuse reflections as follows,

$$\begin{aligned}\mathbf{f}(\mathbf{r}, \theta) &= k_s(\mathbf{r}, \theta)\mathbf{L}\mathbf{o}_w + k_d(\mathbf{r}, \theta)\mathbf{L}\mathbf{o}(\mathbf{r}) \\ &= k_s^{(n)}(\mathbf{r}, \theta)\mathbf{e}_s(\mathbf{r}) + k_d^{(n)}(\mathbf{r}, \theta)\mathbf{e}_d(\mathbf{r}),\end{aligned}\tag{1}$$

where

$$\begin{aligned}\mathbf{e}_s(\mathbf{r}) = \mathbf{e}_s &= \frac{\mathbf{L}\mathbf{o}_w}{\|\mathbf{L}\mathbf{o}_w\|} \\ \mathbf{e}_d(\mathbf{r}) &= \frac{\mathbf{L}\mathbf{o}(\mathbf{r})}{\|\mathbf{L}\mathbf{o}(\mathbf{r})\|} \\ \mathbf{o}_w &= [1, \dots, 1]^T \\ k_s^{(n)}(\mathbf{r}, \theta) &= k_s(\mathbf{r}, \theta) \|\mathbf{L}\mathbf{o}_w\| \\ k_d^{(n)}(\mathbf{r}, \theta) &= k_s(\mathbf{r}, \theta) \|\mathbf{L}\mathbf{o}(\mathbf{r})\|,\end{aligned}$$

$k_s^{(n)}(\mathbf{r}, \theta)$ and $k_d^{(n)}(\mathbf{r}, \theta)$ represent the intensities of specular and diffuse reflections, \mathbf{e}_s and $\mathbf{e}_d(\mathbf{r})$ are the normalized vectors representing the spectral information of each reflection, respectively. In this model, $k_s^{(n)}(\mathbf{r}, \theta)$ and $k_d^{(n)}(\mathbf{r}, \theta)$ depend on the geometry of illuminating angle and visual point from the surface normal vector, \mathbf{e}_s and $\mathbf{e}_d(\mathbf{r})$ are dependent on wavelength only. If these parameters are obtained, we can simulate color reproduction of the object under arbitrary illuminants, illuminating angle, and visual points as described later.

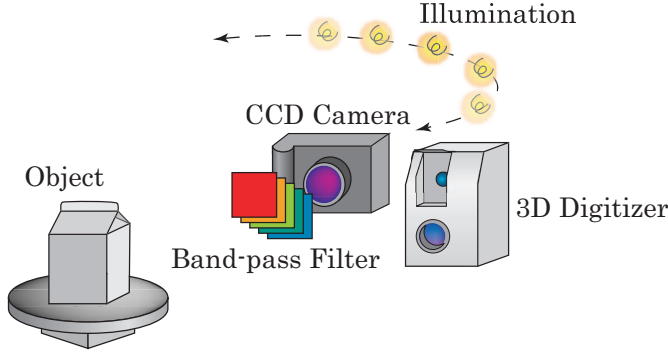


Figure 3: Gonio-photometric image acquisition system.

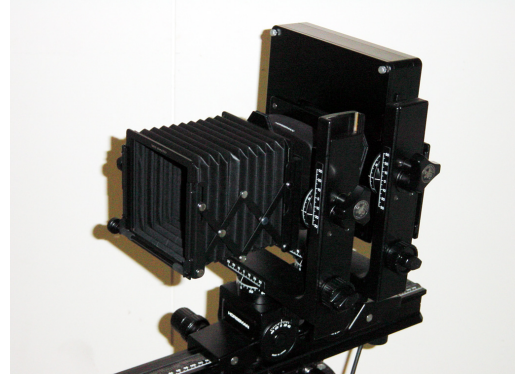


Figure 4: Developed multi-spectral camera.

2.2. Gonio-photometric Model

In recent years, several gonio-photometric models considered with bidirectional reflectance distribution function (BRDF) model have been proposed. Torrance and Sparrow^{7,8} proposed BRDF model that includes off-specular caused masking-shadowing effects by micro facets on the surface. Ward⁹ designed a special device with a half-silvered hemisphere and CCD video camera, which can measure a BRDF of anisotropic reflection, and proposed an anisotropic BRDF model based on a Gaussian lobe. Oren and Nayar^{10,11} proposed a model for diffuse reflection. It is considered that the brightness of a rough surface increases as the viewer approaches the illumination direction. However, these gonio-photometric models require a lot of data to estimate its parameters. In our method, Phong model⁶ is used for representing the specular and diffuse reflection intensities, because this model requires small number of parameters, and represents those intensities well. The gonio-photometric intensity under an arbitrary condition is approximated by a continuous function resulted from Phong model fitting. Phong model is given by

$$k'_s(\theta_s) = A_1 \cos^{A_2}(\theta_s) \quad (2)$$

$$k'_d(\theta_d) = B_1 \cos(\theta_d), \quad (3)$$

where A_1 , A_2 , and B_1 are the parameters for magnitude of specular intensity, glossiness and magnitude of diffuse intensity, respectively. θ_s is the angle between the visualizing angle and the perfect mirror-like reflection angle of the illuminant. θ_d is the angle between the surface normal and the illuminating angle.

3. IMAGE ACQUISITION SYSTEM

In this section, we present the image acquisition system for estimating parameters in the model. The parameters \mathbf{e}_s and $\mathbf{e}_d(\mathbf{r})$ are spectral vector, those dimensions are very high, for example, 81 dimensions when the visible wavelength range, 380-780nm, is sampled at interval of 5nm. To simplify measuring the spectral information of object, we decided to capture the images with several bandpass filters and estimate the spectral radiance from the images. The parameters $k_s^{(n)}(\mathbf{r}, \theta)$ and $k_d^{(n)}(\mathbf{r}, \theta)$ are continuous functions of the illuminating and visualizing angle θ . We estimate the parameters for simulating under arbitrary illuminants, illuminating angle, and visual points from the image sequence under several illuminant angles and obtained 3D geometrical conditions. Figure 3 shows multi-angle-illuminating, multi-band-capturing system we have developed. In this system, we capture 5 bands image sequence by illuminating with a tungsten lamp from 7 different directions (from -30 degrees to 30 degrees at interval of 10 degrees). The multi-spectral camera system shown in Figure 4 is able to capture the image with 3056×2032 pixels, 14-bits levels. The filters attached in front of the CCD camera are exchanged automatically. An example of the multi-angle-illuminating image sequence is shown in Figure 5. In this system,

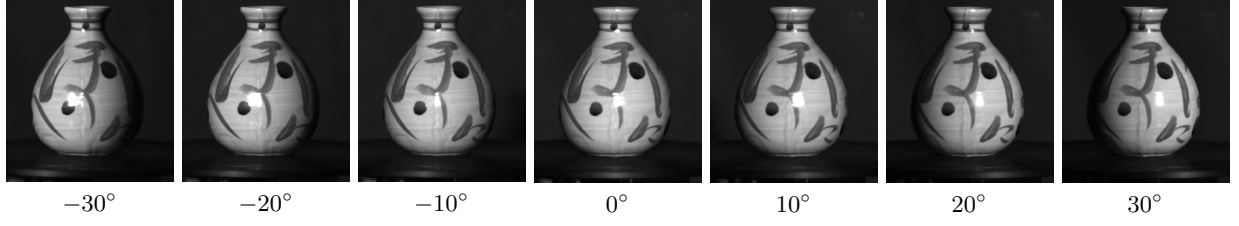


Figure 5: Multi-angle-illuminated image sequence (BPB60).

the multi-band image sequence, $\mathbf{v}(\mathbf{r}, \theta)$, can be represented by,

$$\begin{aligned}\mathbf{v}(\mathbf{r}, \theta) &= \mathbf{S} \mathbf{t}_i \mathbf{f}(\mathbf{r}, \theta) \\ &= \mathbf{H} \mathbf{f}(\mathbf{r}, \theta),\end{aligned}\tag{4}$$

where \mathbf{t}_i is the spectral transmittance of the i th bandpass filter and \mathbf{S} is the spectral sensitivity of the CCD camera. \mathbf{H} denotes a system matrix that consists of spectral sensitivity in the system with \mathbf{S} and \mathbf{t}_i .

We use a 3D digitizer to capture 3D shape of the object. A horizontal stripe laser beam is emitted to the object and produces a bright spot on the object that is imaged by a calibrated CCD camera in the device. The 3D position of the spot is obtained by triangulation. This process is repeated by scanning the stripe light vertically from a top to the bottom of range. A set of obtained 3D points is transformed into 3D surface model for computer graphics applications.

4. DETERMINATION OF MODEL PARAMETERS

After the object data are obtained, we estimate the reflectance properties of the object surface. First, the specular and diffuse components are separated from the multi-band image sequence. Separation of the two reflection components enables us to obtain a reliable estimation of the gonio-photometric parameters, since the gonio-photometric intensities are assumed independent each other. The spectral reflection properties are obtained from the multi-band image.

In Section 4.1 we describe the way to separate the two components from captured multi-band image sequence. In Section 4.2, we explain the approximation of the specular and diffuse intensities based on Phong parameter. Finally, we describe the estimation of the high dimensional spectral reflectance from multi-band images in Section 4.3.

4.1. Separation of Specular and Diffuse Components from Reflected Light

The specular spectral vector \mathbf{e}_s can be determined from a reference white object ($BaSO_4$ plate is used in this experiment.) captured together with the target object, because the specular component has the spectral property that is equivalent to the illuminants. The diffuse spectral vector $\mathbf{e}_d(\mathbf{r})$ is determined as follows. If illuminating angle is varied widely enough, it is supposed that there are illuminating angles at which the reflected light from the object does not include the specular component. In the spectral vector space (see Figure 6), such vector makes its angle from the specular component maximum. Thus, if one finds such a vector and normalize it, it would basically be a unit vector of the diffuse component.

Captured information of spectral radiance $\mathbf{v}(\mathbf{r}, \theta)$ has 5 dimensions, and is obtained by multiplying high dimensional information $\mathbf{f}(\mathbf{r}, \theta)$ and system matrix \mathbf{H} . $\mathbf{v}(\mathbf{r}, \theta)$ is described from Equation (1) and (4) as follows

$$\begin{aligned}\mathbf{v}(\mathbf{r}, \theta) &= \mathbf{H} \mathbf{f}(\mathbf{r}, \theta) \\ &= k_s^{(n)}(\mathbf{r}, \theta) \mathbf{H} \mathbf{e}_s + k_d^{(n)}(\mathbf{r}, \theta) \mathbf{H} \mathbf{e}_d(\mathbf{r}) \\ &= \bar{k}_s^{(n)}(\mathbf{r}, \theta) \bar{\mathbf{e}}_s + \bar{k}_d^{(n)}(\mathbf{r}, \theta) \bar{\mathbf{e}}_d(\mathbf{r}),\end{aligned}\tag{5}$$

where $\bar{\mathbf{e}}_s$ and $\bar{\mathbf{e}}_d(\mathbf{r})$ are the unit vectors in multi-band color space. It is able to calculate the specular and diffuse unit vector $\bar{\mathbf{e}}_s$ and $\bar{\mathbf{e}}_d(\mathbf{r})$ in multi-band color space as well as high dimensional spectral space.

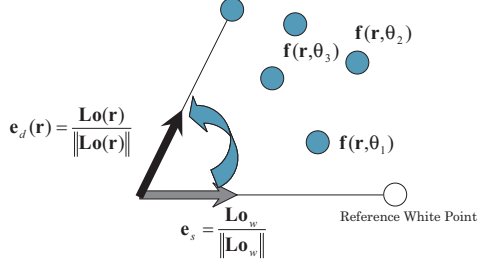


Figure 6. Captured spectral radiances from multi-band image sequence are distributed based on dichromatic model plane.

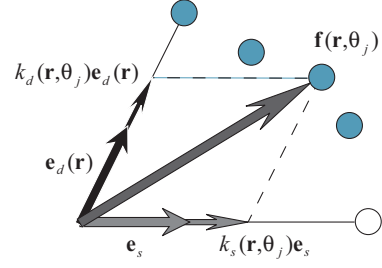


Figure 7. Reflected spectral radiance projected at each spectral vector.

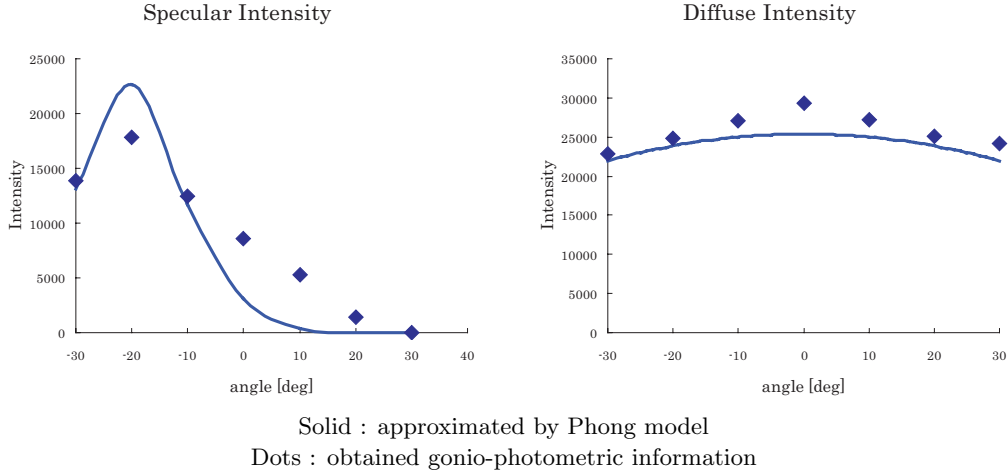


Figure 8: A sample of results of Phong model approximation.

4.2. Approximation of Gonio-photometric Parameters

After determining $\bar{\mathbf{e}}_s$ and $\bar{\mathbf{e}}_d(\mathbf{r})$ as mentioned above, gonio-photometric information $\bar{k}_s(\mathbf{r}, \theta)$ and $\bar{k}_d(\mathbf{r}, \theta)$ are obtained by projecting the reflection component on the each vector $\bar{\mathbf{e}}_s$ and $\bar{\mathbf{e}}_d(\mathbf{r})$ at each illuminating angle θ_j that is the j th illuminating angle. $\bar{k}_s(\mathbf{r}, \theta)$ and $\bar{k}_d(\mathbf{r}, \theta)$ under arbitrary θ are approximated by fitting Phong model given by Equation (2), (3). In this paper, these parameters are determined by a least square fitting using Levenberg-Marquardt method.¹² A sample of the approximation results is shown in Figure 8.

4.3. Estimation of Spectral Reflectance

Estimation of spectral radiance from multi-band images is performed based on multiple regression analysis. The 24 patches of Macbeth ColorChecker were used as the samples for multiple regression analysis. The spectral radiance of each patch was measured by spectrophotometer and corresponding patches of multi-band images were taken. Using multiple regression analysis from Equation (4), the spectral radiance of object is given by

$$\mathbf{f}'(\mathbf{r}, \theta) = \mathbf{H}^- \mathbf{v}(\mathbf{r}, \theta), \quad (6)$$

where the pseudo inverse matrix \mathbf{H}^- is determined so that mean square error between estimation and measurement of spectral radiance is minimized. Explicit form of the pseudo inverse matrix \mathbf{H}^- is given by

$$\mathbf{H}^- = \mathbf{R}_{fg} \mathbf{R}_{gg}^{-1}, \quad (7)$$

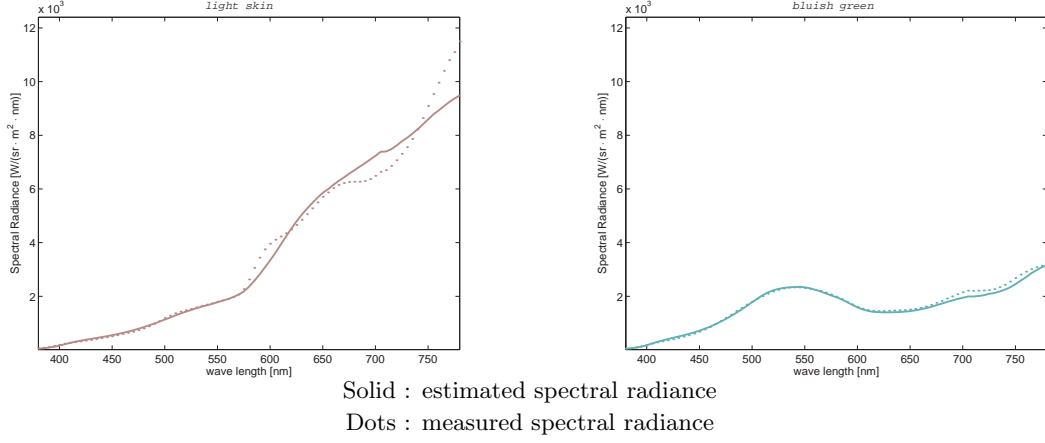


Figure 9: Comparison of the measured and the estimated spectral radiance of color patch of Macbeth ColorChecker.

where \mathbf{R}_{fg} is the correlation matrix between the spectral radiance and the multi-band pixel value while \mathbf{R}_{gg} is the auto-correlation matrix of multi-band pixel value. Accuracy of the multiple regression analysis for two examples shown in Figure 9. The average of color difference ΔE_{94}^* for the 24 patches of Macbeth ColorChecker was 3.79.

5. IMAGE REPRODUCTION EXPERIMENT

Using the captured 3D object shape, the obtained gonio-photometric property parameters, and the estimated spectral reflectance, we can synthesize object images under arbitrary illuminant, illuminating angles, and visual points. This procedure is as follows;

1. The intensities of reflection components $\bar{k}_s(\mathbf{r}, \theta)$ are $\bar{k}_d(\mathbf{r}, \theta)$ are calculated at each surface point \mathbf{r} from the geometric condition of illuminant and visual point θ' of interest.
2. The multi-band value $\mathbf{v}(\mathbf{r}, \theta')$ is determined by $\bar{k}_s(\mathbf{r}, \theta')$, $\bar{k}_d(\mathbf{r}, \theta')$, \bar{e}_s , and $\bar{e}_d(\mathbf{r})$.

$$\mathbf{v}(\mathbf{r}, \theta') = \bar{k}_s(\mathbf{r}, \theta')\bar{e}_s + \bar{k}_d(\mathbf{r}, \theta')\bar{e}_d(\mathbf{r}) \quad (8)$$

3. The spectral radiance $\mathbf{f}'(\mathbf{r}, \theta)$ is estimated by multiplying multiple regression matrix \mathbf{H}^- .

$$\mathbf{f}(\mathbf{r}, \theta') = \mathbf{H}^- \mathbf{v}(\mathbf{r}, \theta') \quad (9)$$

4. The spectral reflectance with gonio-photometric property $\mathbf{o}(\mathbf{r}, \theta')$ is calculated by multiplying the illuminant inverse matrix \mathbf{L}^{-1} that cancels the effect of original illuminant \mathbf{L} .

$$\mathbf{o}(\mathbf{r}, \theta') = \mathbf{L}^{-1} \mathbf{f}(\mathbf{r}, \theta') \quad (10)$$

5. The simulated spectral radiance $\mathbf{f}'(\mathbf{r}, \theta')$ under illuminant \mathbf{L}' of interest is calculated.

$$\mathbf{f}'(\mathbf{r}, \theta') = \mathbf{L}' \mathbf{o}(\mathbf{r}, \theta') \quad (11)$$

6. The tristimulus value $\mathbf{g}(\mathbf{r})$ is obtained by multiplying color matching function \mathbf{T} .

$$\mathbf{g}(\mathbf{r}) = \mathbf{T} \mathbf{f}'(\mathbf{r}, \theta') \quad (12)$$

7. Finally, the image is synthesized by positioning $\mathbf{g}(\mathbf{r})$ on the 3D point \mathbf{r} and rendering it using OpenGL. The precisely simulation color image is reproduced with calibrated display by the tristimulus value image.

Some results of experiment are shown in Figure 10.

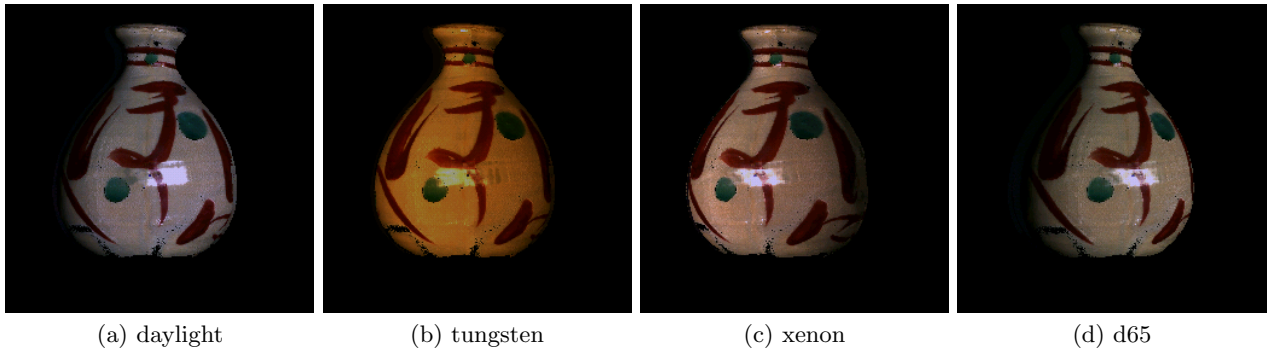


Figure 10: Reproduced images.

6. CONCLUSION

We have developed gonio-photometric imaging system for recording the shape and reflectance property of 3D object by using high accurate multi-spectral camera and 3D digitizer. The gonio-photometric and spectral properties are obtained from the multi-illuminating-angle multi-band image sequence and captured 3D shape. Using the 3D shape, gonio-photometric property, and spectral reflectance property we can synthesize object images under arbitrary illuminants with spectral radiance, illuminating angle, and visual points.

ACKNOWLEDGMENTS

A part of this work was supported by Information-technology Promotion Agency, Japan. Multi-spectral camera was supported by Mitsubishi Electric Micro-Computer Application Software Co., Ltd..

REFERENCES

1. Y. Sato, M. Wheeler, and K. Ikeuchi, "Object shape and reflectance modeling from observation," in *Proceedings of ACM SIGGRAPH 97, in Computer Graphics Proceedings, Annual Conference Series 1997, ACM SIGGRAPH*, pp. 379 – 387, August 1997.
2. H. Haneishi, T. Hasegawa, N. Tsumura, and Y. Miyake, "Design of color filters for recording art works," in *Proceedings of IS & T 50th Annual Conference*, pp. 369–372, 1997.
3. H. Haneishi, T. Iwanami, T. Honma, N. Tsumura, and Y. Miyake, "Color and glossiness reproduction of 3d object surface," *IS & T's PICS Conference, Savannah*, pp. 354–358, 1999.
4. H. Haneishi, T. Iwanami, T. Honma, N. Tsumura, and Y. Miyake, "Goniospectral Imaging of Three-Dimensional Objects," *J. of Imaging Science and Technology*, **45**(5) pp. 451–456, 2001.
5. S. A. Shafer, "Using color to separate reflection components," *Color Research and Application* **10**, pp. 210–218, Win 1985.
6. B. T. Phong, "Illumination for computer generated pictures," *Communications of the ACM* **18**(6), pp. 311–317, 1975.
7. K. E. Torrance and E. M. Sparrow, "Theory for off-specular reflection from roughened surfaces," *Journal of Optical Society of America* **57**(9), 1967.
8. R. L. Cook and K. E. Torrance, "A reflectance model for computer graphics," *ACM Transactions on Graphics* **1**(1), pp. 7–24, 1982.
9. G. Ward, "Measuring and modelling anisotropic reflection," *Computer Graphics* **26**(2), pp 265–272, 1992.
10. M. Oren and S. Nayar, "Generalization of the lambertian model and implications for machine vision," *International Journal of Computer Vision*, **14**, pp 227–251, 1995.
11. K. Dana, B. van Ginneken, S. Nayar, and J. Koenderink, "Reflectance and texture of real-world surfaces," *Technical report, Columbia University*, 1996.

12. W. H. Press, B. P. Flannery, S. A. Teukolsky, and W. T. Vetterling, *Numerical Recipes: The Art of Scientific Computing*, Cambridge University Press, Cambridge, UK, 1986.
13. Y. Miyake, "Development of multiband color imaging systems for recording of art paintings," in *Color Imaging : Proc. SPIE* **3648**, pp. 215–225, 1999.
14. S. Tominaga, "Realization of color constancy using the dichromatic reflection model," In *The second IS & T and SID's Color Imaging Conference*, pp. 37–40. 1994.
15. T. Honma, T. Iwanami, H. Haneishi, N. Tsumura, and Y. Miyake, "Recording and Estimation of Reflection Spectra of 3D Object Based on Dichromatic and Phong Models," *International Symposium on Multispectral Imaging and Color Reproduction for Digital Archives*, pp. 131–134, 1999.